

Discovery of Early Optical Emission from GRB 021211

D. W. Fox¹, P. A. Price^{2,3}, A. M. Soderberg¹, E. Berger¹, S. R. Kulkarni¹, R. Sari⁴,
D. A. Frail⁵, F. A. Harrison², S. A. Yost², K. Matthews¹, B. A. Peterson³, I. Tanaka⁶,
J. Christiansen³ & G. H. Moriarty-Schieven⁷

ABSTRACT

We report our discovery and early time optical, near-infrared, and radio wavelength follow-up observations of the afterglow of the gamma-ray burst GRB 021211. Our optical observations, beginning 21 min after the burst trigger, demonstrate that the early afterglow of this burst is roughly three magnitudes fainter than the afterglow of GRB 990123 at similar epochs, and fainter than almost all known afterglows at an epoch of 1 d after the GRB. Our near-infrared and optical observations indicate that this is not due to extinction. Combining our observations with data reported by other groups, we identify the signature of a reverse shock. This reverse shock is not detected to a $3\text{-}\sigma$ limit of $110\ \mu\text{Jy}$ in an 8.46-GHz VLA observation at $t = 0.10$ d, implying either that the Lorentz factor of the burst $\gamma \lesssim 200$, or that synchrotron self-absorption effects dominate the radio emission at this time. Our early optical observations, near the peak of the optical afterglow (forward shock), allow us to characterize the afterglow in detail. Comparing our model to flux upper limits from the VLA at later times, $t \gtrsim 1$ week, we find that the late-time radio flux is suppressed by a factor of two relative to the $\gtrsim 80\ \mu\text{Jy}$ peak flux at optical wavelengths. This suppression is not likely to be due to synchrotron self-absorption or an early jet break, and we suggest instead that the burst may have suffered substantial radiative corrections.

Subject headings: galaxies: high-redshift – gamma rays: bursts

¹Caltech Optical Observatories 105-24, California Institute of Technology, Pasadena, CA 91125

²Space Radiation Laboratory, 220-47, California Institute of Technology, Pasadena, CA 91125

³Research School of Astronomy and Astrophysics, Mount Stromlo and Siding Spring Observatories, via Cotter Road, Weston Creek 2611, Australia

⁴Theoretical Astrophysics 130-33, California Institute of Technology, Pasadena, CA 91125

⁵National Radio Astronomy Observatory, Socorro, NM 87801

⁶Astronomical Institute, Tohoku University, Sendai, 980-8578, Japan

⁷National Research Council of Canada, Joint Astronomy Centre, 660 N. A'ohoku Place, Hilo, HI 96720

1. Introduction

Gamma-ray burst (GRB) afterglow emission on timescales of hours to days, the historical standard for ground-based follow-up observations, can provide a robust measure of the global parameters of the GRB such as its total explosive yield and the density of the circumburst medium on length scales of $r \gtrsim 10^{17}$ cm (Sari et al. 1998; Wijers & Galama 1999).

Early emission, on a timescale of tens of minutes and less, can offer insight into the details of the explosion, including the relativistic Lorentz factor of the burst ejecta (Sari & Piran 1999b) and the distribution of the circumburst medium on length scales $r \gtrsim 10^{15}$ cm. If the GRB progenitor is a massive star, then this regime is expected to show the clear signature of a dense stellar wind (density $\rho \propto r^{-2}$; Chevalier & Li 2000).

These two unique diagnostics, among others, have motivated searches for early optical emission from GRBs. The first success came with detection of early optical (Akerlof et al. 1999) and radio (Kulkarni et al. 1999) emission from GRB 990123 (Briggs et al. 1999). This emission has been interpreted in terms of a reverse shock plowing back through the GRB ejecta (Sari & Piran 1999a; Mészáros & Rees 1999).

After nearly four years, early emission was recently discovered again from GRB 021004 (Fox et al. 2003) and GRB 021211 (Fox & Price 2002). These discoveries were made possible by the prompt alerts of the *HETE-2* satellite (Ricker et al. 2002), and the wide field and high sensitivity of the 48-inch Palomar Oschin Schmidt telescope (P48) equipped with the NEAT camera (Pravdo et al. 1999). The increase in the number of robotic telescopes has allowed for intensive follow-up of both of these bursts during the critical early minutes to hours. Here, we report the discovery of early optical emission and subsequent multi-wavelength follow-up observations of GRB 021211.

2. Observations

GRB 021211 (HETE Trigger #2493) was detected at UT 11:18:34 on 11 Dec 2002. With a duration of 6 s and a fluence (8–40 keV) of 10^{-6} erg cm $^{-2}$, the event is a typical long duration GRB (Crew et al. 2002). At the time of electronic notification the *HETE-2* localization, although large (30-arcminute radius), was covered by the $1.1^\circ \times 1.1^\circ$ field-of-view of NEAT. We identified a new source that was not present in the Palomar Sky Survey (Fig. 1) and announced this as a possible optical counterpart of GRB 021211 (Fox & Price 2002). The best *HETE-2* localization at the time of our discovery announcement was 14 arcmin in radius; a subsequent SXC localization produced the 2 arcmin-radius circle

shown in Figure 1. The position of the optical transient (OT) with respect to the Guide Star Catalog II is $\alpha=08:08:59.858$ and $\delta=+06:43:37.52$ (J2000) with estimated uncertainty of 0.1 arcsec in each axis.

We continued monitoring with P48, the 40-inch telescope at Siding Spring (SS0-40), and the Palomar Hale 5-m (P200) telescope with JCAM (Bloom et al. 2003). Photometry has been performed using the secondary calibrators of Henden (2002); see Table 1.

Our optical source was subsequently identified in images obtained by several robotic telescopes and other ground-based facilities. In particular, RAPTOR (Wozniak et al. 2002), KAIT (Li et al. 2002) and S-LOTIS (Park et al. 2002) detected the source 90 s, 108 s, and 143 s after the burst, respectively. In Figure 2 we present the light curve obtained by combining data from these and other GCNs with our data (Table 1).

Near-infrared – We observed the afterglow in the near-infrared with the Cassegrain f/70 infrared camera and D-78 detector (Soifer et al. 1991) on P200 on Dec. 11.55 UT (K_s band) and with NIRC (Matthews & Soifer 1994) on the Keck-I 10-m telescope on Dec. 18.5 UT (JHK_s). NIRC observations were photometered relative to SJ 9116 and SJ 9134 (Persson et al. 1998), and the P200 zero-point was determined from the NIRC observations by reference to two secondary calibrators, S1 and S2 (see Fig. 1). Our results are given in Table 1.

Radio – We searched for radio emission with the Very Large Array (VLA)⁸; our initial observation at $t = 2.44$ hr represents the earliest radio observation of any GRB to date. We used PKS 0734+100 for phase calibration and 3C 147 and 3C 286 for flux calibration. No counterpart to the OT is detected in any single observation. Adding the data between 2002 December 20 and 2003 January 6, we measure an 8.46-GHz upper limit of $35 \mu\text{Jy}$ at the position of the OT. Peak flux densities at the position of the OT can be found in Table 2.

Separately, on Dec 12.51 UT we carried out an observation in the 347-GHz band with the Submillimetre Common User Bolometer Array (SCUBA) on the James Clerk Maxwell Telescope (JCMT)⁹. We used CRL 618 as the secondary flux standard. At the position of the OT we measure a 347-GHz flux density of $2.0 \pm 2.5 \text{ mJy}$.

⁸The NRAO is a facility of the National Science Foundation operated under cooperative agreement by Associated Universities, Inc.

⁹The James Clerk Maxwell Telescope is operated by The Joint Astronomy Centre on behalf of the Particle Physics and Astronomy Research Council of the United Kingdom, the Netherlands Organization for Scientific Research, and the National Research Council of Canada.

3. A Two-Component Light Curve

To date, only three bursts have had early-time optical detections: GRB 990123 (Akerlof et al. 1999), GRB 021004 (Fox et al. 2003) and GRB 021211. GRB 021211 is at any epoch one of the faintest detected afterglows; at early epochs it is more than 3 mag fainter than GRB 990123, and at later epochs ($t \gtrsim 1$ d) it lies below the great majority of afterglow lightcurves (Fig. 2). As we show below, this is not the result of extinction in the host galaxy, so this burst reminds us that many so-called “dark bursts” may simply be faint (c.f. Fynbo et al. 2001; Berger et al. 2002).

Examining Figure 2, we see that the early behavior of GRB 021211 bears a striking resemblance to the light curve of GRB 990123 (c.f. also Chornock et al. 2002). The light curve can be considered as composed of two segments: an initial steeply-declining “flash”, $f \propto t^{-\alpha}$ with $\alpha_{\text{rs}} \sim 1.6$, followed by emission declining as a typical afterglow, $\alpha_{\text{fs}} \sim 1$. The corresponding terms are “flare” and afterglow for the radio emission (Kulkarni et al. 1999).

The optical flash is thought to result from a reverse shock propagating into the GRB ejecta (Sari & Piran 1999a), whereas the afterglow arises in the shocked ambient material swept up by the ejecta (Sari et al. 1998). For each shock, it is assumed that some fraction of the shock energy is partitioned into energetic electrons (ϵ_e) and magnetic fields (ϵ_B). The electrons are expected to follow a power-law distribution in energy, $dN/d\gamma \propto \gamma^{-p}$ for $\gamma > \gamma_m$, where γ is the electron Lorentz factor. Their collective emission follows $f_\nu \propto \nu^{-(p-1)/2}$ at frequencies above the synchrotron peak frequency ν_m and $f_\nu \propto (\nu/\nu_m)^{1/3}$ otherwise. Below the self-absorption frequency ν_a , synchrotron self-absorption becomes important, and above the characteristic cooling frequency ν_c , electrons lose their energy rapidly, on the timescale of the shock evolution.

The evolution of the forward and reverse shocks are different. Once the reverse shock has passed through the ejecta shell then no new electrons are accelerated and the shocked electrons cool adiabatically: $\nu_m \propto t^{-73/48}$, with the flux at ν_m (the “peak” flux) decaying as $F_{\nu_m} \propto t^{-47/48}$ (Sari & Piran 1999b). Furthermore, the emission for $\nu > \nu_c$ decreases even more rapidly. In contrast, electrons are continually added to and accelerated at the forward shock, so that F_{ν_m} (for a uniform circumburst medium) is constant, and even above the cooling frequency the flux declines only slowly. Since in a stellar wind-type ($\rho \sim r^{-2}$) circumburst medium the reverse shock ν_c is inevitably below the optical band, detection of long-lived reverse shock emission for GRB 021211 suffices to rule out wind models for this burst (Chevalier & Li 2000).

3.1. The Reverse Shock Flare

The optical flux is already declining at the first epoch (RAPTOR; Woźniak et al. 2002), when $t = t^* = 90$ s and $R_c = 14$ mag, corresponding to $f = f^* = 7.7$ mJy at a mean frequency of $\nu_o = 4.7 \times 10^{14}$ Hz – here the superscript * identifies quantities taken at $t = 90$ s. This implies that $\nu_m^* < \nu_o$, and constrains the time when the flare spectral peak ν_m passes through the optical bandpass, $t_{m,o}$, to be $t_{m,o} < t^*$. Since the observed decline at $t > t^*$ is not very rapid, $\alpha_{rs} \lesssim 2$, we have also that $\nu_c^* > \nu_o$.

The constraint on the time of the optical peak flux can be converted into a constraint on the relativistic Lorentz factor γ of the GRB ejecta. From Sari & Piran (1999b) we have $t_{\text{peak}} = 5 n_0^{-1/3} \gamma_{300}^{-8/3} E_{52}^{1/3}$ s (thin-shell case), where t_{peak} is the time at which the reverse shock crosses the GRB ejecta, n_0 is the circumburst particle density per cubic cm, γ_{300} is $\gamma/300$, and E_{52} is the isotropic-equivalent burst energy in units of 10^{52} erg. Since $t_{\text{peak}} < t_{m,o} < t^*$, we find that $\gamma > 100 n_0^{-1/8} E_{52}^{1/8}$.

Using the prompt emission fluence of $\mathcal{F}_\gamma \sim 10^{-6}$ erg cm $^{-2}$ in the 8–40 keV band (Crew et al. 2002) together with the proposed redshift of $z = 1.006$ (Vreeswijk et al. 2002), we find an isotropic γ -ray energy of $E_{\text{iso}} = 3 \times 10^{51}$ ergs for GRB 021211. Since this fluence is measured over a relatively narrow band, the full k -corrected fluence (Bloom et al. 2001) may easily reach 10^{52} ergs, so it is reasonable to assume $E_{52} \sim 1$.

Following Sari & Piran (1999a), in the absence of synchrotron self-absorption the radio flux will follow $F_r \propto t^{-17/36}$ for times $t < t_{m,r}$, and $F_r \propto t^{-\alpha_{rs}}$ for times $t > t_{m,r}$, where $t_{m,r}$ is the time when ν_m passes through the radio band, $\nu_r = 8.5$ GHz. The value of $t_{m,r}$ follows directly from the equation $t_{m,r} = t_{m,o} (\nu_o/\nu_r)^{48/73}$, and is equal to 1.35 d in the limiting case $t_{m,o} = t^*$. By this time the peak flux will have declined as $F_{m,r} = F_{m,o} (t_{m,r}/t_{m,o})^{-47/48}$. Note that we are temporarily ignoring extinction effects, which will selectively suppress the optical flux relative to the radio; this is discussed in §3.2 below.

For $t_{m,o} < t^*$, we extrapolate the observed optical flux decay back in time as $F_{m,o} = f^*(t_{m,o}/t^*)^{-\alpha_{rs}}$. The light curve of the radio flare is thus a direct function of $t_{m,o}$:

$$F_r(t \leq t_{m,r}) = 8.9 \times 10^{-4} f^* \left(\frac{t_{m,o}}{t^*} \right)^{-\alpha_{rs}} \left(\frac{t}{t_{m,r}} \right)^{-17/36}, \quad (1)$$

with the decay past $t_{m,r}$ steepening to $t^{-\alpha_{rs}}$. Our 3- σ upper limits at $t = 0.10$ d and $t = 0.92$ d are 110 μ Jy and 66 μ Jy, respectively. For $\alpha_{rs} \approx 1.6$ (§3.2), the radio flux at $t = 0.92$ d is relatively insensitive to $t_{m,o}$, and is predicted to be about 15 μ Jy. In the absence of self-absorption, however, the radio flux at $t = 0.10$ d is a strong function of $t_{m,o}$, and Eq. 1 gives $t_{m,o} > 20$ s and $F_{m,o} < 135$ mJy.

A lower limit on $t_{m,o}$ implies an upper limit on the Lorentz factor of the ejecta, $\gamma < 180n_0^{-1/8} E_{52}^{1/8}$. Following the treatment of Sari & Piran (1999a), however, we find that synchrotron self-absorption may be suppressing the radio flux below the level of Eq. 1, which would render this limit invalid.

3.2. The Forward Shock Afterglow

A variety of afterglow lightcurves are possible (Kobayashi 2000) but the form of sharp rise, plateau, and power-law decay is near-universal. Given the bright flare, we cannot constrain the rising portion of the afterglow lightcurve. We fit the flare as a power-law decay of index α_{rs} and the afterglow as a constant flux, f_m , which undergoes a power-law decay with index α_{fs} for $t > t_b$ (Fig. 2).

We first examine the constraints on the reverse shock decay. Published GCN data are sufficient to constrain $\alpha_{rs} = 1.63 \pm 0.13$, and since $\alpha_{rs} = \frac{47}{48} + \frac{73}{48}(\frac{p-1}{2})$ (Sari & Piran 1999a), this implies that $p = 1.85 \pm 0.17$.

The gap between the GCN data and our P48 measurements creates fitting degeneracies in the full model, so we fix α_{rs} at three successive values, 1.50, 1.63, and 1.76, and make fits to the full dataset. Incorporating the range in parameter uncertainties covered in these three fits, we find that $\alpha_{fs} = 0.80 \pm 0.13$, $f_m = 65 \pm 20 \mu\text{Jy}$ and $t_b = 1700 \pm 280 \text{ s}$. Note that because the flare dominates the afterglow emission at early times, our fitted f_m should be considered a lower limit and our t_b an upper limit.

In addition to α_{fs} , we measure the power-law slope of the spectrum, $\beta_{\text{obs}} = -0.98$ using our B and K_s photometry near $t = 0.1 \text{ d}$ (correcting first for Galactic extinction of $A_r=0.07 \text{ mag}$; Schlegel et al. 1998). If $\nu_c < \nu_o$ at this time, then $\alpha_{fs} = 3/4(p - 1) + 1/4$, $p = 1.7 \pm 0.2$, and $\beta = -p/2 = -0.85 \pm 0.1$, implying little extinction in the host, $A_R = 0.15 \pm 0.18$ in the observer frame. On the other hand, if $\nu_c > \nu_o$ at this time, then $\alpha_{fs} = 3/4(p - 1)$, $p = 2.1 \pm 0.2$, and $\beta = -(p - 1)/2 = -0.55 \pm 0.1$, corresponding to an intrinsic reddening of $A_R = 0.48 \pm 0.18$ (observer frame). In either case, extinction within the host cannot explain the $\sim 2 \text{ mag}$ gap between the R -band lightcurve and those of most afterglows.

Since we do not know the location of ν_c relative to the optical band, we adopt an average extinction correction of $A_R = 0.3$. This corrects our limiting peak flux of $f_m \gtrsim 65 \mu\text{Jy}$ to an unextinguished flux of $F_m \gtrsim 85 \mu\text{Jy}$.

From our model fits, $\alpha_{fs} = 0.8 \pm 0.13$, so that $F_m \approx 85(t_{m,o}/t_b)^{-0.8} \mu\text{Jy}$. We can use this relation along with Eqs. 4.3 and 4.5 of Sari & Esin (2001) to estimate the circumburst density

on length scales of $r \sim 2\gamma^2 t_b c \lesssim 10^{18}$ cm. We find that $n_0 = 0.1\epsilon_{B,-2}^{-23/15} \epsilon_{e,-1}^{-32/15} E_{52}^{-38/15} \text{ cm}^{-3}$, where $\epsilon_e = 0.1\epsilon_{e,-1}$. Since we have $E_{52} \sim 1$ (§3.1), this implies either a low density circumburst medium, or abnormally low values of ϵ_B or ϵ_e .

In the absence of self-absorption, the radio afterglow can be expected to peak at time $t \lesssim t_b(\nu_o/\nu_r)^{48/73} \lesssim 25$ d. In the standard model the synchrotron peak flux F_m remains constant as the peak frequency decreases, so we expect a radio peak flux of roughly $85 \mu\text{Jy}$. Prior to the peak time, $\nu_r < \nu_m$ and $F_r \sim t^{0.5}$. At the mean epoch of our summed image, $t = 17.3$ d, we expect $F_r \sim 70 \mu\text{Jy}$, and our $2\text{-}\sigma$ upper limit is $F_r < 35 \mu\text{Jy}$, a factor of two below the predicted level.

We can estimate the self-absorption frequency (Eq. 4.1 of Sari & Esin 2001) in terms of the peak flux, $\nu_a = 0.7 E_{52}^{-9/20} n_0^{3/20} (F_m/85 \mu\text{Jy})^{1.86}$ GHz. Self-absorption will be effective in the case of a high circumburst density – unlikely on the basis of our n_0 estimate – or if F_m is sufficiently large. In the latter case, at fixed frequency the effects of increasing self-absorption win out over the raw increase in flux. Suppressing the radio flux by a factor of two requires $F_m \gtrsim 800 \mu\text{Jy}$ ($t_{m,o} \lesssim 100$ s), however, which seems unlikely.

The discrepancy between the observed and expected fluxes can be due to an early jet break, $t_{\text{jet}} < t_{m,r}$ (Rhoads 1999; Sari et al. 1999). The optical light-curve, however, shows no sharp steepening out to $t \gtrsim 10$ d (Fig. 2). Moreover, the measured fluence and proposed redshift $z = 1.006$ for GRB 021211 are consistent with minimal beaming for a “standard candle” burst ($E_{\text{iso}} \sim 5 \times 10^{50}$ ergs; Frail et al. 2001), so that an early jet-break seems an unlikely scenario to explain the suppression of the radio flux.

Alternatively, the afterglow radiative corrections (Sari 1997; Cohen et al. 1998) may be significant. In the slow-cooling regime ($\nu_c > \nu_m$), radiative corrections can be substantial if ϵ_e is large ($\epsilon_e \gtrsim 0.1$), ν_c is close to ν_m , or p is close or equal to 2. We have not derived an estimate for ϵ_e , but $p \approx 2$ for our models, so this scenario remains an attractive candidate for future modeling.

Acknowledgments.

We acknowledge the efforts of the NEAT team at JPL, and of Scott Barthelmy at Goddard for the GCN. Thanks are due to Josh Bloom, who has built an excellent transient observing system in JCAM. SRK thanks S. Thorsett for maintaining the “hyperlinked GCN” web page. GRB research at Caltech is supported by grants from NSF and NASA.

REFERENCES

- Akerlof, C. et al. 1999, *Nature*, 398, 400
- Berger, E. et al. 2002, *ApJ*, 581, 981
- Bloom, J. S., Frail, D. A., & Sari, R. 2001, *AJ*, 121, 2879
- Bloom, J. S., Kulkarni, S. R., Clemens, J. C., Diercks, A., Simcoe, R. A., & Behr, B. B. 2003, *Publ. Astr. Soc. Pacific*, submitted
- Briggs, M. S. et al. 1999, *Astrophys. J.*, 524, 82
- Chevalier, R. A. & Li, Z. 2000, *Astrophys. J.*, 536, 195
- Chornock, R., Li, W., Filippenko, A. V., & Jha, S. 2002, *GRB Circular Network*, 1754, 1
- Cohen, E., Piran, T., & Sari, R. 1998, *ApJ*, 509, 717
- Crew, G. et al. 2002, *GRB Circular Network*, 1734, 1
- Fox, D. W. & Price, P. A. 2002, *GRB Circular Network*, 1731, 1
- Fox, D. W. et al. 2003, *Nature*, submitted
- Frail, D. A. et al. 2001, *ApJ*, 562, L55
- Fruchter, A., Levan, A., Vreeswijk, P., Holland, S. T., & Kouveliotou, C. 2002, *GRB Circular Network*, 1781, 1
- Fynbo, J. U. et al. 2001, *A&A*, 369, 373
- Henden, A. 2002, *GRB Circular Network*, 1753, 1
- Kobayashi, S. 2000, *ApJ*, 545, 807
- Kulkarni, S. R. et al. 1999, *Astrophys. J.*, 522, L97
- Li, W., Filippenko, A. V., Chornock, R., & Jha, S. 2002, *GRB Circular Network*, 1737, 1
- Mészáros, P. & Rees, M. J. 1999, *Mon. Not. R. astr. Soc.*, 306, L39
- Matthews, K. & Soifer, B. T. 1994, *Experimental Astronomy*, 3, 77
- Park, H. S., Williams, G., & Barthelmy, S. 2002, *GRB Circular Network*, 1736, 1

- Persson, S. E., Murphy, D. C., Krzeminski, W., Roth, M., & Rieke, M. J. 1998, *AJ*, 116, 2475
- Pravdo, S. H. et al. 1999, *Astron. J.*, 117, 1616
- Rhoads, J. E. 1999, *ApJ*, 525, 737
- Ricker, G. et al. 2002, *ApJ*, 571, L127
- Sari, R. 1997, *ApJ*, 489, L37+
- Sari, R. & Esin, A. A. 2001, *ApJ*, 548, 787
- Sari, R. & Piran, T. 1999a, *Astrophys. J.*, 517, L109
- 1999b, *Astrophys. J.*, 520, 641
- Sari, R., Piran, T., & Halpern, J. P. 1999, *ApJ*, 519, L17
- Sari, R., Piran, T., & Narayan, R. 1998, *ApJ*, 497, L17+
- Schlegel, D. J., Finkbeiner, D. P., & Davis, M. 1998, *ApJ*, 500, 525
- Soifer, B. T. et al. 1991, *ApJ*, 381, L55
- Vreeswijk, P., Fruchter, A., Hjorth, J., & Kouveliotou, C. 2002, *GRB Circular Network*, 1785, 1
- Wijers, R. A. M. J. & Galama, T. J. 1999, *ApJ*, 523, 177
- Wozniak, P. et al. 2002, *GRB Circular Network*, 1757, 1

Table 1. Optical Photometry for GRB021211

Date (UT)	ΔT (days)	Telescope	Filter	Magnitude	Error
Dec 11.4854	0.0144	P48	R ^a	18.293	0.024
Dec 11.4962	0.0252	P48	R ^a	18.813	0.045
Dec 11.4997	0.0287	P48	R ^a	19.093	0.059
Dec 11.5064	0.0354	P48	R ^a	19.343	0.071
Dec 11.5120	0.0410	P48	R ^a	19.286	0.068
Dec 11.5139	0.0429	P48	R ^a	19.479	0.077
Dec 11.5218	0.0508	P48	R ^a	19.529	0.082
Dec 11.5251	0.0541	P48	R ^a	19.598	0.086
Dec 11.5270	0.0560	P48	R ^a	19.755	0.102
Dec 11.5332	0.0622	P48	R ^a	19.950	0.110
Dec 11.5399	0.0689	P48	R ^a	20.091	0.130
Dec 11.6025	0.1310	SSO40/WFI	B	21.877	0.138
Dec 11.7083	0.2370	SSO40/WFI	R	21.096	0.128
Dec 11.5533	0.0823	P200/IRcam	Ks	18.01	0.150
Dec 12.518	1.037	P200/JCAM	g'	23.398	0.047
Dec 12.518	1.037	P200/JCAM	r'	23.416	0.073
Dec 18.49	7.019	K-I/NIRC	Ks	22.12	0.18
Dec 18.52	7.049	K-I/NIRC	J	22.77	0.11
Dec 18.56	7.089	K-I/NIRC	H	22.48	0.16

^aP48 unfiltered observations have been photometered against the *R*-band calibration of Henden (2002).

Table 2. Radio Observations of GRB 021211

Date (UT)	ΔT (days)	Telescope	Frequency (GHz)	Flux (μJy)	Flux Error (μJy)
2002 Dec 11.57	0.10	VLA	8.46	12	36
2002 Dec 12.39	0.92	VLA	8.46	–36	22
2002 Dec 13.40	1.93	VLA	8.46	9	45
2002 Dec 13.40	1.93	VLA	22.5	48	62
2002 Dec 15.32	3.85	VLA	8.46	45	23
2002 Dec 16.29	4.82	VLA	8.46	–6.5	19
2002 Dec 20.32	8.85	VLA	8.46	60	28
2002 Dec 22.26	10.79	VLA	8.46	0.3	27
2002 Dec 26.44	14.97	VLA	8.46	–7.3	23
2002 Dec 28.55	17.08	VLA	8.46	33	28
2003 Jan 04.39	23.92	VLA	8.46	2.4	24
2003 Jan 06.28	25.81	VLA	8.46	46	24
Dec 20–Jan 06		VLA	8.46	15	10

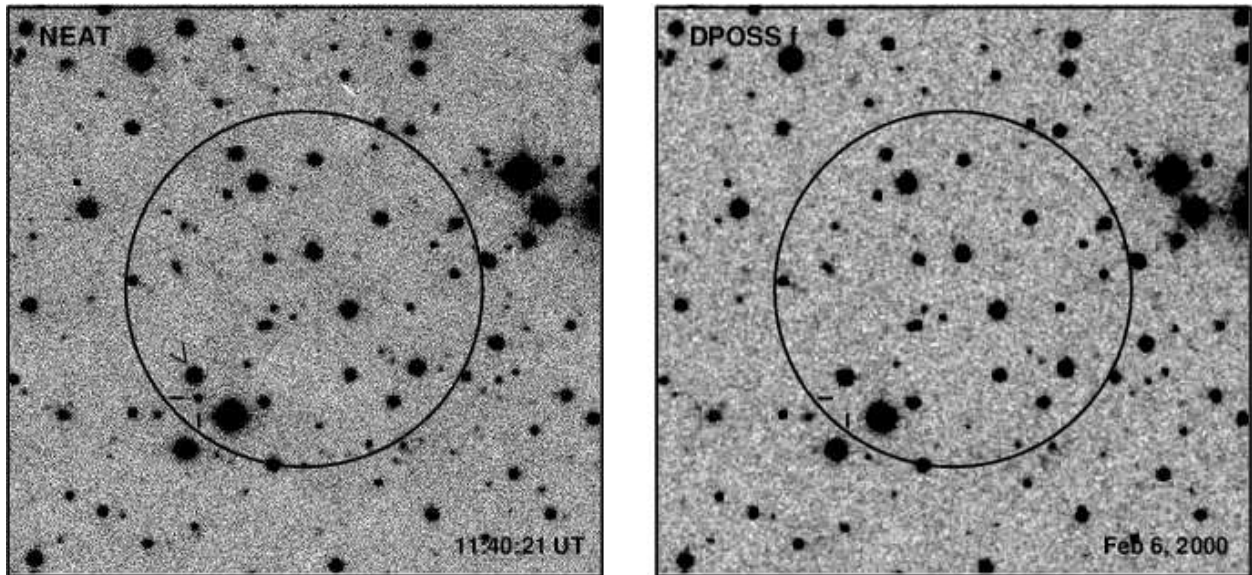


Fig. 1.— Discovery image of the optical afterglow of GRB021211, as obtained with the Near Earth Asteroid Tracking (NEAT) camera on the Oschin 48-inch telescope, Palomar Observatory, 21 min after the burst (left). The R -band (f-emulsion) Palomar Digital Sky Survey (DPOSS) image of the GRB localization region is shown for comparison (right). The afterglow is marked by two dashes. The circle of radius 2 arcminutes marks the subsequent SXC localization. The position of S1, one of our secondary standards for NIR photometry (§2), is indicated by a carat on the NEAT image; S2 is not visible in either image. Coordinates of S1 are $\alpha=08:09:00.0$, $\delta=+06:43:52$ (J2000) and coordinates of S2 are $\alpha=08:09:00.3$, $\delta=+06:43:38$ (J2000).

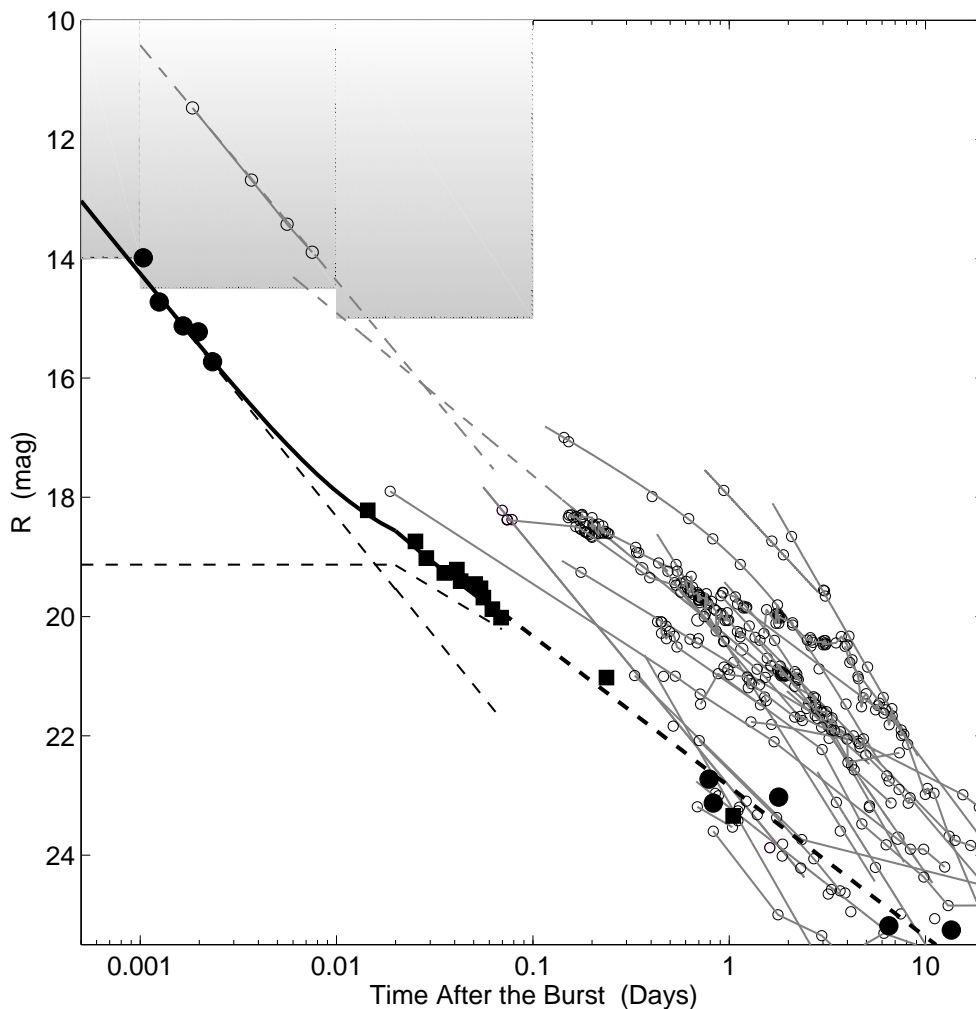


Fig. 2.— Light curve of GRB 021211 and other GRBs, including a two-component flare + afterglow fit for the early optical emission from GRB 021211. The data for GRB 021211 are drawn from the GCN literature (circles; see text) and this work (squares; Table 1). We fit the data at $t < 0.1$ d only (see §3.2 for details); the dotted line at $t > 0.1$ d is merely illustrative. The last two points ($t > 5$ d) are derived from HST observations (Fruchter et al. 2002) and should be largely free of host contamination. The data for other GRBs are drawn from the literature (see Berger et al. 2002).